Simulation of Continuous Deodorizers: Effects on Product Streams

Roberta Ceriani and Antonio J.A. Meirelles*

LASEFI (Physical Separation Laboratory), Food Engineering Department, State University of Campinas (UNICAMP), Cidade Universitária Zeferino Vaz, Campinas, São Paulo, Brazil, 13083-970

ABSTRACT: This work deals with the simulation of deodorization, one important process in the edible oil industry related to the removal of odoriferous compounds. The deodorizer was modeled as a multicomponent stripping-column in cross-flow and countercurrent flow. The impact of processing parameters on the quality of the product streams was analyzed. The deodorization of soybean and canola oils (plant scale) and wheat germ oil (lab-scale) was studied under typical ranges of temperature, stripping steam rate, and pressure. Their entire compositions were considered within the simulations, including acylglycerols, FFA, and other key components such as tocopherols and sterols. The deodorization results were analyzed in terms of retention of tocopherol and sitosterol and of neutral oil loss to the distillate. The deodorizer modeling considered Murphree efficiencies and entrainment for each plate. A case study, i.e., the deodorization of soybean oil, illustrated the applicability of our modeling.

Paper no. J10889 in *JAOCS 81,* 1059–1069 (November 2004).

KEY WORDS: Countercurrent flow, cross-flow, deodorization, entrainment, multicomponent stripping, Murphree efficiency, neutral oil loss, simulation, tocopherol retention, vegetable oils.

Deodorization is a steam-stripping process responsible for vaporizing odoriferous compounds and FFA from the oil, carrying them to the distillate, and producing edible oil. Although it targets only these undesirable compounds, other components with comparable volatilities are also lost (1).

Since deodorizer operating conditions are based on oil quality rather than distillate concerns, a vaporization of tocopherols and sterols occurs in the course of deodorization, even though these components are less volatile than FFA (2). The economical importance of these compounds is related to their value to the food and chemical industries: Tocopherols are natural antioxidants and are considered a quencher of free radicals (3), whereas sterols are used in the manufacture of pharmaceuticals, such as hormones and corticoids (2). As pointed out by Ahrens (3), different markets pose different quality demands. Although the economic value of the distillate depends on its composition and content of tocopherols and sterols (4), some markets, such as in Europe, are concerned with the retention of tocopherols in the refined oil (3). In the United States, the deodorization temperature is set up to 270°C, since it is important to recover tocopherol in the distillate (3).

This work deals with the evaluation by process simulation of the impact of processing parameters on the quality and composition of the finished oil and, as a consequence, of the deodorization distillate. We selected three different vegetable oils for this study: soybean oil, because it is widespread; genetically modified canola oil rich in oleic acid; and wheat germ oil, because of its unique composition that is rich in PUFA and tocopherols (5).

The continuous deodorizers (plant- and laboratory-scale) were modeled as a multicomponent stripping column, following the method described by Naphtali and Sandholm (6). Group contribution methods were selected to calculate all the physical properties needed in the equilibrium relationships and energy balances.

Soybean oil was presumed to contain TAG, DAG, and MAG; FFA; δ-tocopherol; squalene; and β-sitosterol (7). Wheat germ oil was assumed to have TAG, DAG, and MAG; FFA; and α-tocopherol (5). Canola oil was characterized by TAG, DAG, and MAG; FFA; and γ-tocopherol (8). Note that we considered a representative tocopherol and sitosterol to identify the whole class of these compounds. Pryde (7) and Woerfel (2) found that the main sitosterol and the main tocopherol in soybean oil are, respectively, β-sitosterol and δ-tocopherol. For wheat germ oil, α-tocopherol is the representative tocopherol (5). In canola oil, γ-tocopherol is the main tocopherol (8).

MODELING CONTINUOUS DEODORIZERS: PLANT AND LABORATORY

In commercial deodorization, two relevant flow patterns are used: cross-flow (Fig. 1A), which implies that the flow directions of the phases cross each other, and countercurrent flow, in which the inlet of the gas is at the outlet of the oil, and the outlet of the gas is at the inlet of the oil (9). Thin-film deodorizers are based in the countercurrent contact between gas and oil (9). Lab-scale continuous tray deodorizers, such as the one used by Wang and Johnson (5) for wheat germ oil, also use a countercurrent flow (Fig. 1B).

Modeling of the multicomponent stripping column was based on the method described by Naphtali and Sandholm (6). The general equations, which include material and energy balances and Murphree efficiencies coupled with vapor–liquid

*To whom correspondence should be addressed.
E-mail: tomze@fea.unicamp.br (A.J.A. Meirelles)

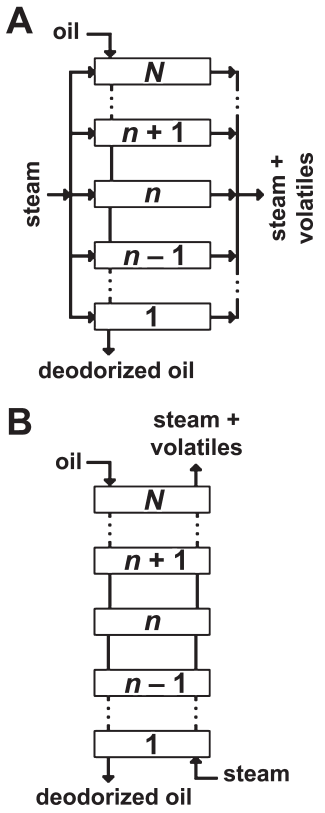

FIG. 1. Continuous tray design: (A) cross-flow and (B) countercurrent flow.

equilibrium (VLE) relationships, are described briefly in Appendices I and II. An iterative procedure (Newton–Raphson) is used for simultaneous convergence until the true values of $l_{n,i}$ (the component liquid molar flow), $v_{n,i}$ (the component vapor molar flow), and T (the temperature) corresponding to each stage are found. Input data to the calculations were as follows: (i) identification and division of the mixture components in usual groups and the respective parameters, according to each group contribution method selected; (ii) specification of the processing variables: number of stages, Murphree efficiencies, feed location and composition, flow pattern (cross-flow or countercurrent), feed flow rates and thermal states, and column pressure; and (iii) initial estimation for the total molar flow rates for each stage and for the temperature profile.

To express the VLE found in each tray, the thermodynamic approach of Ceriani and Meirelles (10), which considers the nonideality of the vapor and liquid phases, was applied. Their VLE approach is shown below:

$$k_i = \frac{y_i}{x_i} = \frac{\gamma_i \cdot f_i^0}{P \cdot \phi_i} \quad [1]$$

where

$$f_i^0 = P_i^{vp} \cdot \phi_i^{sat} \cdot \exp\left(\frac{V_i^L \cdot (P - P_i^{vp})}{R \cdot T}\right) \quad [2]$$

where f_i^0 is the standard-state fugacity; x_i and y_i are the molar fractions of component i in the liquid and vapor phases, respectively; P is the total pressure; R is the gas constant; T is the system absolute temperature; P_i^{vp} and ϕ_i^{sat} are, respectively, the vapor pressure and the fugacity coefficient of the pure component i; γ_i is the liquid-phase activity coefficient; ϕ_i is the vapor-phase fugacity coefficient; and V_i^L is the liquid molar volume of component i. The exponential term corresponds to the Poynting factor (POY). As shown in Appendices I and II, this correlation is valid for each stage n, corrected by the Murphree efficiency. The vapor pressure P_i^{vp} and the activity coefficient γ_i are calculated for each fatty compound using, respectively, the group-contribution approach developed by Ceriani and Meirelles (10) and the UNIFAC $r^{3}/_{4}$ (11). Various works in the area of the VLE of fatty mixtures (10,11) have confirmed that UNIFAC (UNIquac Functional group Activity Coefficient) $r^{3}/_{4}$ better suits the prediction of the liquid-phase behavior.

Equations 1 and 2 describe the VLE rigorously. Previous works (10,11) have demonstrated that some simplifications may be applied in the analysis of oil–solvent mixtures. POY and ϕ_i are nearly one, whereas ϕ_i^{sat} deviates notably from unity for compounds whose vapor pressures are very high at the system temperature, such as water, short-chain FA, and *n*-hexane. A good investigation of the nonidealities of fatty mixtures can be found in Ceriani and Meirelles (10).

ESTIMATION OF OIL COMPOSITION, PHYSICAL PROPERTIES, MURPHREE EFFICIENCIES, AND ENTRAINMENT

Soybean, canola, and wheat germ oils are formed by TAG, DAG, and MAG in addition to a variety of other minor compounds. This work, in particular, is concerned with the behavior of fatty components (FA and acylglycerols), tocopherols, and sterols within the deodorization process. To estimate their entire composition in terms of TAG, we used the methodology suggested by Antoniosi Filho *et al.* (12), which is based in a statistical procedure that considers lipase hydrolysis characteristics. In this way, the TAG compositions were estimated from the FA compositions given by Firestone (8) for soybean oil, by Rabelo *et al.* (13) for canola oil, and by Wang and Johnson (5) for wheat germ oil. The composition in DAG and MAG was obtained from the estimated TAG composition in the following way: Each TAG was split into 1,2- and 1,3-DAG; each DAG was then split into MAG following the stoichiometric relations of the prior compounds (TAG in the case of DAG, and DAG in the case of MAG). The same considerations were previously applied successfully by Ceriani and Meirelles (14) to estimate coconut oil composition (15) in the evaluation of batch physical refining by simulation, and by Rabelo *et al.* (13) to predict kinematic viscosities. The tocopherol, squalene, and β-sitosterol concentrations in soybean oil were taken from Pryde (7) and Maza *et al.* (16). The tocopherol concentration in canola oil was taken from Firestone (8). The tocopherol concentration in wheat germ oil was given by

Wang and Johnson (5). Compounds responsible for odors and flavors were not included in the oil composition, given that the residual FFA content can be used as an indicator of odor elimination (1).

Pertinent information on the general composition of soybean, canola, and wheat germ oils is shown in Table 1. As a whole, the wheat germ oil had 7 FFA (Table 1), 22 TAG, 11 DAG, and 5 MAG. The main TAG were PLiLi (18.0%, w/w), POLi (10.3%, w/w), LiLiLi (22.8%, w/w), and OLiLi (18.2%, w/w), where P = palmitate, Li = linoleate, O = oleate, and Ln = linolenate. PLi–, LiLi–, and OLi– were the key DAG (27.7, 27.0, and 22.1%, respectively). The MAG class was formed mainly by O— (19.1%), P— (20.4%), and Li— (55.7%). The complete composition of acylglycerols for the soybean oil is shown in Table 2. The complete TAG composition for the canola oil can be found by referring to Rabelo *et al.* (13). Its key TAG were OOLi (24.3%, w/w), OOO (24.0%, w/w), and OOLn (17.8%, w/w). OO– (44.7%, w/w) and O— (69.4%, w/w) were the main DAG and MAG, respectively.

Because of the high number and large diversity of compounds found in the deodorizer, predictive group contribution methods were selected to estimate all the physical properties required for the enthalpy balance and equilibrium conditions. To calculate activity coefficients, UNIFAC $r^{3}/_{4}$ was used (11). Fugacity coefficients were calculated using the virial equation (19). Critical properties and acentric factors of the pure components, needed to calculate second virial coefficients, were estimated using the well-known Joback technique for critical volumes and pressures, and Fedor's group contributions for critical temperatures (19). For the energy balances, vapor and liquid heat capacities and enthalpies of vaporization are required. We selected Joback's technique for ideal vapor heat capacities, Rowlinson–Bondi's method for liquid heat capacities (19), and the method of Tu and Liu (20) to estimate the enthalpy of vaporization of each compound involved. The physical properties of water (stripping steam) were calculated using equations from the Design Institute for Physical Properties (DIPPR®) Chemical Database (21). To predict the vapor pressure of squalene, we selected the method of Voutsas *et al.* (22). Required inputs are the normal boiling temperature and the respective liquid density, which were calculated using the methods of Retzekas *et al.* (23) and Elbro *et al.* (24), respectively. Equation 3 was obtained from the direct use of these methods on squalene. For β-sitosterol, the empirical equation suggested

TABLE 1
General Composition of Soybean, Wheat Germ, and Canola Oils

FA	Trivial name (abbreviation)	Soybean oil mass (%)[a]	Wheat germ oil mass (%)[b]	Canola oil mass (%)[c]
C14:0	Myristic (M)	—	—	0.10
C16:0	Palmitic (P)	9.7	16.3	6.79
C16:1	Palmitoleic (Po)	—	—	0.33
C18:0	Stearic (S)	5.4	0.9	1.83
C18:1	Oleic (O)	25.0	18.2	60.99
C18:2	Linoleic (Li)	52.4	56.5	21.01
C18:3	Linolenic (Ln)	5.5	6.0	8.48
C20:0	Arachidic (A)	0.6	0.2	0.32
C20:1	Gadoleic (G)	0.2	1.9	—
C20:2	Gadolenic (Gn)	0.1	—	—
C22:0	Behenic (Be)	0.7	—	—
C22:1	Erucic (E)	0.2	—	0.15
C24:0	Lignoceric (Lg)	0.2	—	—

Class of compounds	Mass (%)	*M* (g/gmol)	Mass (%)	*M* (g/gmol)	Mass (%)	*M* (g/gmol)
TAG	99.300	875.27	96.6831	869.07	99.376	875.68
DAG	0.146	612.05	2.6000[d]	606.60	0.200	612.98
MAG	0.004	352.03	0.3000[d]	349.58	0.005	352.43
FFA	0.070[e]	279.37	0.1700[b]	277.07	0.100[f]	279.80
Squalene	0.014[g]	410.72	—	—	—	—
β-Sitosterol	0.330[g]	414.72	—	—	0.250[a]	414.72
Tocopherol	0.136[e]	414.00	0.2469[b]	414.00	0.070[a]	414.00
M.W.	864.61		848.26		867.18	
Iodine value (IV)	126.34		128.98		110.99	
IV ranges[a]	118–139		115–128		110–126	

[a] From Firestone (8).
[b] Same composition of bleached wheat germ oil, from Wang and Johnson (5).
[c] From Rabelo *et al.* (13).
[d] From Barnes (17).
[e] From Maza *et al.* (16).
[f] From Eskin *et al.* (18).
[g] From Pryde (7).

TABLE 2
Estimated Composition of Soybean Oil

	TAG			DAG		
Group[a]	Major TAG	M^b (g/gmol)	Mass (%)	Acylglycerol compound	M^b (g/gmol)	Mass (%)
50:1	POP	832	0.78	PP–	568	1.25
52:1	POS	860	0.82	PS –	596	0.44
54:1	SOS	888	0.31	SS–	624	0.17
56:1	POBe	916	0.15	PLg–	680	0.06
58:1	POLg	944	0.10	PO–	594	5.91
50:2	PLiP	830	1.44	SO–	622	5.86
52:2	POO	858	3.94	OA –	650	0.73
54:2	SOO	886	1.86	OBe–	678	0.57
56:2	PLiBe	914	0.46	OLg –	706	0.08
58:2	OOBe	942	0.36	PLi –	592	16.85
60:2	OOLg	970	0.14	OO–	620	8.63
50:3	PLnP	828	0.16	LiA–	648	0.43
52:3	POLi	856	9.16	LiBe –	676	0.43
54:3	SOLi	884	6.75	LiLg –	704	0.20
56:3	OLiA	912	0.72	PLn –	590	1.18
58:3	OLiBe	940	0.66	OLi –	618	32.62
60:3	OLiLg	968	0.31	LiG–	646	0.22
52:4	PLiLi	854	9.28	LiE–	674	0.18
54:4	OOLi	882	15.41	LiLi –	616	21.33
56:4	LiLiA	910	0.77	LiGn–	644	0.07
58:4	LiLiBe	938	0.77	LiLn –	614	2.79
60:4	LiLiLg	966	0.30		MAG	
52:5	PLiLn	852	1.84	P—	330	13.10
54:5	OLiLi	880	21.56	S—	358	3.33
56:5	LiLiG	908	0.40	O—	356	31.59
58:5	LiLiE	936	0.32	Li—	354	48.42
60:5	LiLnLg	964	0.06	Ln—	352	2.00
52:6	PLnLn	850	0.10	A—	386	0.60
54:6	LiLiLi	878	16.29	G—	384	0.11
56:6	LiLiGn	906	0.13	Gn—	382	0.03
54:7	LiLiLn	876	4.21	Be—	414	0.53
54:8	LiLnLn	874	0.44	E—	412	0.10
				Lg—	442	0.19

[a]Isomer set including different TAG, but all with the same number of FA carbons and double bounds. For example, Group 50:1 refers to the isomer set of TAG with 50 FA carbons and one double bond.
[b]*M*, M.W. (g/gmol). For other abbreviations see Table 1.

by Bokis *et al.* (25) was applied. For tocopherol, we adjusted an equation for the curve of vapor pressure vs. temperature shown by Woerfel (2). This last step was taken to overcome the inadequacy of group contribution methods (22) in predicting the vapor pressure of tocopherols. It is important to highlight that, in this way, we were capable of describing the existing relations among the volatilities of the minor compounds considered: squalene > tocopherol > sitosterol (2,4). In this way, Equation 4 was developed to predict the vapor pressure of tocopherol. Note that Equation 4 has the same form for the dependence between the logarithm of the vapor pressure and temperature as Bokis *et al.* (25) suggested for sitosterol (Eq. 5).

$$\ln P^{vp}_{squalene}\,(\text{Pa}) = 101325 \cdot \frac{T(\text{K}) - 733.14}{T(\text{K}) - 121.2966} \quad [3]$$

$$\ln P^{vp}_{tocopherol}\,(\text{Pa}) = 21.44191 - \frac{191754.2}{T^{1.5}(\text{K})} \quad [4]$$

$$\ln P^{vp}_{sitosterol}\,(\text{Pa}) = 20.75045 - \frac{199959.3}{T^{1.5}(\text{K})} \quad [5]$$

Other properties of these compounds were calculated using the aforementioned methods.

For the vapor–liquid separation process, considering that both liquid and vapor phases are mixed perfectly, a measure of the efficiency of mass transfer for a component *i* on the *n*th stage is the Murphree efficiency (26). As suggested by Ludwig (26), the Murphree efficiency (η) can be estimated with the user-friendly equations of MacFarland *et al.* (27) as a function of dimensionless groups: the surface tension number N_{Dg}, the liquid Schmidt number N_{Sc}, and the modified Reynolds number N_{Re}. The two models developed by the authors for the traditional hydrocarbon and chemical industries are given below:

$$\eta = 7.0 \cdot (N_{Dg})^{0.14} \cdot (N_{Sc})^{0.25} \cdot (N_{Re})^{0.08} \quad [6]$$

$$\eta = 6.8\,(N_{Re} \cdot N_{Sc})^{0.1} \cdot (N_{Dg} \cdot N_{Sc})^{0.115} \quad [7]$$

$$N_{Dg} = \sigma_L/\mu_L \cdot U_{VN};\ N_{Sc} = \mu_L/\rho_L \cdot D_{LK};\ N_{Re} = \rho_V \cdot U_{VN} \cdot h_w/\mu_L \cdot \text{FA} \quad [8]$$

where σ_L is the surface tension of the liquid (lb/h^2), μ_L is the liquid viscosity (lb/h·ft), U_{VN} is the vapor superficial velocity (ft/h), ρ_L and ρ_V are the liquid and vapor densities (lb/ft^3), respectively, h_w is the weir height (ft), FA is the fractional free area (the ratio of the fractional area of the holes to the column free cross-sectional area), and D_{LK} is the liquid diffusivity (ft^2/h) at infinite dilution from the Wilke–Chang equation (19). Surface tensions and diffusivities were calculated using the well-known methods of Reid *et al.* (19). Viscosities and densities were calculated according to Rabelo *et al.* (13) and Halvorsen *et al.* (28), respectively. As pointed out by Carlson (1), for properly designed deodorizers, U_{VN} is usually less than 2 m/s.

All $\eta_{n,i}$ values (Murphree efficiencies for each component at each tray; see Appendices I and II) were considered equal to η (Eqs. 6–8), which is a simplifying approximation. To calculate η, we considered a typical load of soybean oil (4,425 kg/h) at 3 mm Hg, 260°C, and 1% of stripping steam. The mixture involved in this calculation was characterized by pseudo-compounds: an equivalent TAG (same M.W. and unsaturation of the oil), an equivalent FFA (same M.W. and unsaturation of the oil acidity), and water. The calculated values of η for soybean oil were 57.15% using Equation 6 and 46.91% using Equation 7. For wheat germ oil, η was 53.65% using Equation 6 and 44.64% using Equation 7. For comparison purposes we also calculated η for palm oil (752 g/gmol): The values obtained were 61.68 and 49.99%, respectively, for Equations 6 and 7. As one can see, η ranged from 54 to 62% for Equation 6, and from 45 to 50% (more conservative) for Equation 7. For simplicity, $\eta_{n,i} = 0.50$ was chosen to represent the Murphree efficiency in our work. The approximation of the whole multicomponent mixture by an equivalent

ternary one, containing pseudo-compounds, was used only in the case of efficiency estimation.

Mechanical entrainment of oil is defined as the carrying of oil droplets in the vapor upward from the free surface to the outlet of the equipment (1). In industrial deodorizers, losses of neutral oil by entrainment are believed to be around 0.1–0.2%, with an additional loss of about 10% of the FFA amount in the feed (1). To account for the mechanical entrainment in our simulations, we used the graphical method of Fair and Mathews (see Ref. 26) for bubble-cap and perforated plates. This correlation was developed on the basis of a flow parameter $[L_n/V_n \cdot (\rho_V/\rho_L)^{0.5}]$ and a capacity parameter $[U_{VN} \cdot (\rho_V/\rho_L - \rho_V)^{0.5}]$. It relates the percentage of flood, the fractional entrainment ψ (moles of liquid entrained/moles of liquid downflow), liquid and vapor flow rate, and the densities of the vapor and liquid. The ψ value from our calculations was 0.024 mol of liquid entrained/mol of liquid downflow. The entrainment term, e_n (moles of liquid entrained/moles of vapor), of Equations A1 and A2 and of Equations A6 and A7 is related to ψ by the following equation (26):

$$e_n = \frac{\psi}{1-\psi} \cdot \frac{L_n}{V_n} \quad [9]$$

In particular, for countercurrent flow tray deodorizers, part of the liquid of lower concentration of the plate below $(n-1)$ is entrained and carried by the vapor to the plate above (n), reducing its liquid concentration with respect to the more volatile compounds. As a consequence, the vapor rising from this plate (n) will be of lower concentration, reducing the net amount of mass transfer and the efficiency as well. The Murphree efficiency must be corrected to take this effect into account (26). The wet Murphree efficiency, η_w, can be easily calculated as a function of ψ (26):

$$\eta_w = \eta / \left(1 + \eta \cdot \frac{\psi}{1-\psi}\right) \quad [10]$$

All $\eta_{n,i}$ values in the equilibrium relationships of the countercurrent deodorizer (see Appendix I) were considered equal to η_w. For cross-flow deodorizers, $\eta_{n,i}$ values (see Appendix II) were set as equal to η.

For the countercurrent deodorizer (laboratory-scale), the pressure drops of the trays were added so that the pressure at the bottom of the column was two to three times the top pressure (29). For cross-flow deodorizers, the pressure drop was negligible.

RESULTS AND DISCUSSION

We now present the results obtained in our deodorization simulations following processing parameter ranges found in the literature: oil load (kg/h), percentage of stripping steam, temperature, and pressure. To evaluate the industrial deodorization of soybean and canola oil, we followed the directions given by Maza *et al.* (16), Ahrens (3), Eskin *et al.* (18), and Brekke (30). In the case of the laboratory-scale deodorization of wheat germ oil, we were guided by the work of Wang and Johnson (5), in which a laboratory-scale continuous countercurrent deodorizer of 15 trays (as in Fig. 1B) was used. Murphree efficiencies and entrainment were also inputs for the program simulations. Table 3 shows the processing parameters studied in this work. As one can see, the combination of these parameters led to a considerable number of possibilities for simulation. In the case of soybean oil, two sets of simulation conditions were studied; the first one was related to the

TABLE 3
Operating Conditions for the Continuous Deodorizer Simulations

Parameter	Soybean oil (plant scale, cross-flow)		Canola oil (plant scale, cross-flow)	Wheat germ oil[a] (lab scale, countercurrent)
Stripping steam	880 lb/h (399.2 kg/h)[b,c]	1.0, 1.3 and 2.0%[c,d,e]	1.3 and 2.0%[c,d,e,f]	0.25 cm^3 of water/min[g] (0.015 kg/h)
Temperature (°C)	246, 253, and 260[b] (475, 488, and 500°F)	242, 250, and 258[e]	240, 250, and 260[f]	200 and 250
Oil load	40,000, 45,000, and 50,000 lb/h[b] (18,144, 20,412, and 22,680 kg/h)	4,425 kg/h[e]	4,425 kg/h[e]	10 and 25 mL/min (0.5 and 1.2 kg/h)
Top pressure (mm Hg)	4[b]	1, 2.775 (3.7 mbar), and 6[e]	1, 2.5, and 4[f]	5
Pressure drop	Negligible	Negligible	Negligible	0.36 mm Hg per tray[h]
Number of trays	3[e]	3[e]	3[e]	15
Murphree efficiency ($\eta_{n,i}$)	0.50	0.50	0.50	0.494[i]
Entrainment (e_n)[j]	0.4324	0.4324	0.4324	0.4324

[a]From Wang and Johnson (5).
[b]From Maza *et al.* (16).
[c]The stripping steam is distributed equally in each stage of the column (Fig. 1A).
[d]Calculated as the percentage of total oil load.
[e]From Ahrens (3) and Brekke (30). The oil feed is introduced into the column at the top stage (third).
[f]From Eskin *et al.* (18).
[g]The stripping steam is fed at the bottom as a single stream (Fig. 1B).
[h]Following the directions of Stage (29).
[i]Murphree efficiency corrected for entrainment for stage *n* and component *i*.
[j]Entrainment for each stage *n* (moles of liquid entrained/moles of vapor).

work of Maza *et al.* (16). The most significant results are discussed below.

From the parameters given in Table 3, we selected a typical deodorization of soybean oil from Ahrens (3) (2.775 mm Hg, 1.3% of stripping steam, and 250°C) to explore and discuss some of the results given by the simulation program. Figure 2 shows the profiles of the mass fraction of FFA, acylglycerol, squalene, tocopherol, and sterol curves in the liquid and vapor phases within the column. As expected, the FFA concentration in the liquid phase (Fig. 2A) dropped off from the feed third stage to the first stage. The total acylglycerol concentration (including TAG, DAG, and MAG) did not change significantly, since the TAG concentration prevailed over DAG and MAG in the liquid oil. The squalene, tocopherol, and sterol curves had slight variations, but as is shown later, these changes were significant when compared with the feed concentration of each compound. As shown in Figure 2B, the vapor phase formed at the top stage was richer in acylglycerols, FFA, and squalene than the vapor phase formed at the bottom. Given that the steam fed at the third stage was in contact with the oil feed, there was a stronger driving force for mass transfer. Figure 2C shows the profiles of liquid and vapor flows (mol/h) and enthalpies (kJ/h) for each stage. Since the difference between temperatures at the top and the bottom of the column was less than 0.1°C (249.96 and 249.91, respectively), and stripping steam was injected at each stage, the enthalpies did not change considerably.

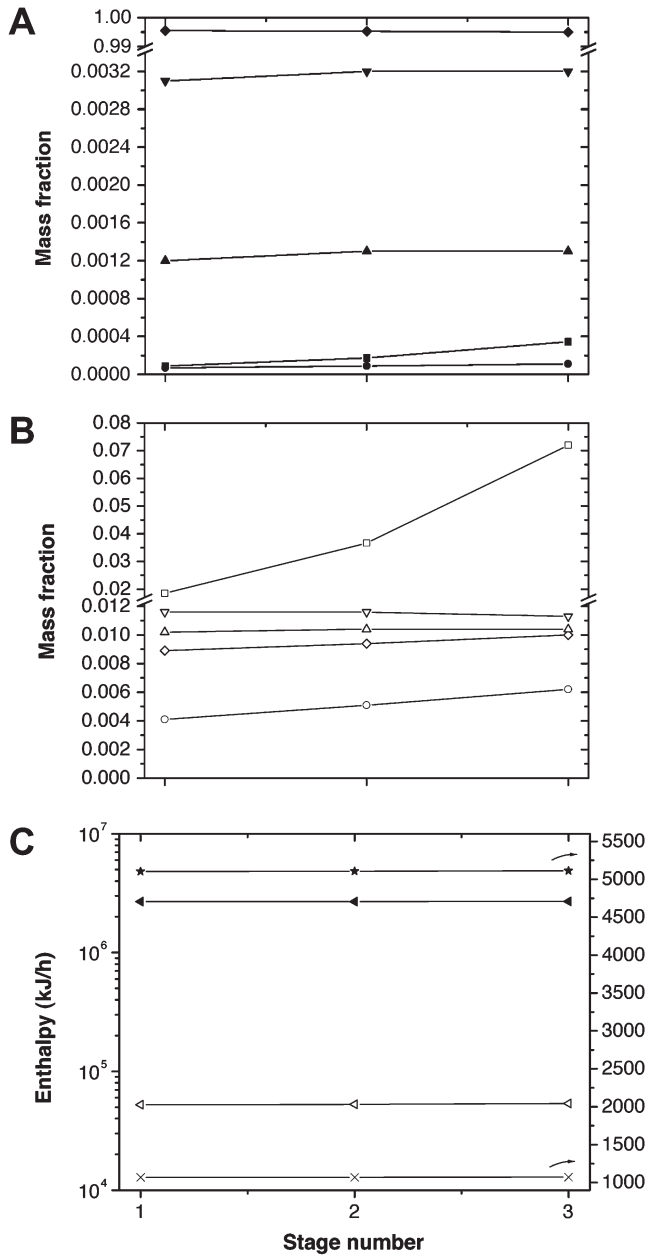

FIG. 2. Profiles for the mass fractions of acylglycerols, FFA, squalene, β-sitosterol, and δ-tocopherol (A) in the liquid phase and (B) in the vapor phase; (C) enthalpies and flows for a typical deodorizing condition (3). (◆) Liquid phase acylglycerols, (■) FFA, (▼) β-sitosterol, (▲) δ-tocopherol, and (●) squalene. (◇) Vapor phase acylglycerols, (□) FFA, (▽) β-sitosterol, (△) δ-tocopherol, and (○) squalene. Liquid (◀) and vapor (◁) enthalpies. Liquid (★) and vapor (×) flows.

To analyze the results of our methodology, we also studied the influence of the processing conditions on the quality of the product streams, i.e., the deodorized oil and the distillate. As already discussed, the optimized conditions for operating a deodorizer depend on the composition of the oil at the inlet of the deodorizer (neutralized or bleached oil) and the desired compositions of the products. Table 4 shows selected values of the deodorizer distillate as a function of temperature and pressure, obtained with 1.3% of stripping steam. As expected, the distillate flow increased with temperature and decreased with system pressure. Neutral oil loss (NOL) followed the same statement, since the volatility of acylglycerols rose at higher temperatures. Because of entrainment, acylglycerols became the main fraction of the distillate. Simulation results (250°C and 2.775 mm Hg, as an example in Table 4), including entrainment effects, led to a considerable increase in NOL values (0.01 to 0.06%), especially of TAG content in the distillate (7.14 to 85.08%, in a free basis of water). Walsh *et al.* (31) explain that a good indication of excess neutral oil in the distillate is the ratio of the acid value to the saponification value. According to the authors, this parameter should be ≥0.67. Looking at Table 4, we can see that, in the simulation that considers entrainment, this value is equal to 0.09. As pointed out by Carlson (1), entrainment separators are capable of preventing the mechanical carryover of oil droplets, thereby reducing entrainment losses to less than 0.1–0.2%. An additional loss by distillation also occurs and is usually lower than 0.1% for nonlauric oils (1). Distillate compositions in terms of minor compounds (squalene, tocopherol, and β-sitosterol) and their recovery are also expressed in Table 4. Depending on temperature and pressure conditions, important quantities of tocopherol and β-sitosterol were present in the distillate. As an example, for temperatures greater than 250°C, our simulations showed that, depending on the system pressure, it was possible to recover between 7 and 35% of the initial tocoph-erol in the distillate. At 242°C, this value was lower than 20% even at 1 mm Hg. For a typical deodorization condition (250°C and 2.775 mm Hg), the tocopherol and sitosterol retentions were

TABLE 4
Composition of the Deodorizer Distillate (%) of Soybean Oil and the Corresponding Final Oil Acidity for Different Temperatures and Pressures[a,b]

	1 mm Hg			2.775 mm Hg				6 mm Hg		
					250°C					
Class of compounds	242°C	250°C	258°C	242°C	With entrainment	Without entrainment	258°C	242°C	250°C	258°C
TAG	7.40	11.62	17.57	4.45	85.08	7.14	11.25	3.24	5.08	7.96
DAG	2.68	3.63	4.68	1.63	0.47	2.27	3.11	1.19	1.62	2.22
MAG	2.27	1.93	1.56	2.55	0.39	2.48	2.28	2.44	2.50	2.49
Squalene	6.91 (74.8%)[c]	6.02 (82.0%)	4.97 (87.7%)	6.68 (43.4%)	1.01 (52.1%)	6.47 (51.8%)	6.04 (60.2%)	5.84 (24.1%)	5.77 (30.1%)	5.64 (36.9%)
β-Sitosterol	19.65 (9.0%)	22.33 (12.9%)	24.03 (18.0%)	12.26 (3.4%)	2.52 (5.5%)	14.50 (4.9%)	16.65 (7.0%)	9.03 (1.6%)	10.46 (2.3%)	12.05 (3.3%)
δ-Tocopherol	17.12 (19.1%)	18.84 (26.4%)	19.43 (35.3%)	11.20 (7.5%)	2.14 (11.3%)	13.08 (10.8%)	14.76 (15.1%)	8.38 (3.6%)	9.65 (5.2%)	11.02 (7.4%)
FFA	43.96	35.62	27.77	61.22	8.39	54.06	45.90	69.88	64.90	58.62
Distillate (kg/h)	6.70	8.44	10.94	4.02	31.97	4.96	6.17	2.56	3.23	4.04
NOL (%)[d]	0.02	0.03	0.06	0.01	0.06	0.01	0.02	0.004	0.007	0.01
Tocopherol (mg/kg)[e]	1,104	1,004	884	1,260	1,215	1,216	1,157	1,313	1,291	1,261
Oil acidity (%)[f]	0.0029	0.0015	0.0008	0.0137	0.0089	0.0089	0.0055	0.0288	0.0219	0.0158
Ratio AV/SV[g]	0.79	0.69	0.55	0.89	0.09	0.83	0.75	0.92	0.89	0.83

[a]1.3% of stripping steam. Murphree efficiencies were considered.
[b]Concentration expressed as g/100 g of distillate, in a free basis of water.
[c]Numbers in parentheses are the compound recovery in the distillate, expressed in percentage (%).
[d]Neutral oil loss (NOL) calculated in relation to the total oil feed (4,425 kg/h).
[e]Tocopherol content in the deodorized oil.
[f]Expressed as percentage of oleic acid (% C18:1) in the deodorized oil.
[g]Ratio of acid value (AV) to saponification value (SV) (31).

89.2 and 95.1%, respectively. Ahrens (3) reported a tocopherol retention of 76% for soybean oil for the same condition, although the initial contents of FFA and tocopherol were different (0.06% and 1,120 mg/kg, respectively). For this simulation, the initial FFA content was 0.07%, and the initial tocopherol content was 1,360 mg/kg, which can explain the relatively higher tocopherol retention. In general, as the system temperature increased, the deodorizer distillate became richer in TAG, DAG, tocopherol, and β-sitosterol. On the other hand, an increase in the system pressure led to a reduction in the fractions of TAG, DAG, tocopherol, and β-sitosterol. A high degree of tocopherol recovery (>20%), which enhances the economical value of the distillate (3), is possible to attain by controlling the deodorization conditions. In general, lowering the system pressure allowed the recovery of higher concentrations of tocopherol and β-sitosterol in the distillate. Walsh *et al.* (31) indicated that, for optimal tocopherol recovery, temperatures should be above 260°C. To exemplify this statement, we simulated a condition of 2.775 mm Hg and 274°C, with 1.3% of stripping steam. In this case, 27.6% of tocopherol could be recovered in the distillate.

Most of the results presented in Table 4 do not include losses due to entrainment (or mechanical carryover), but only losses due to distillation. For a better understanding of these two effects, we separated them in Figure 3. At 250°C and 2.775 mm Hg, vaporization was the main cause of squalene, tocopherol, and β-sitosterol losses. On the other hand, almost all NOL was due to entrainment.

In relation to deodorizer distillate composition, our simulations showed that, apart from the temperature and pressure effects, TAG, DAG, MAG, and FFA contents ranged from 3.2 to 17.6%, from 1.2 to 4.7%, from 1.6 to 2.6%, and from 27.8 to 69.9%, respectively. For squalene, β-sitosterol, and tocopherol contents, the ranges within the distillate were from 5.0 to 6.9%, from 9.0 to 24.0%, and from 8.4 to 19.4%, in that order. In the GC analysis of two different deodorizer distillate samples of soybean oil, Verleyen *et al.* (4) found the following composition: 5.1 and 5.9% of TAG, 2.7 and 3.8% of DAG, 1.2 and 1.9% of MAG, 32 and 33% of FFA, 1.3 and 2.1% of squalene, 7.9 and 8.3% of sitosterol, and 16.5 and 18.0% of tocopherols. Roughly, these results fit between the ranges obtained

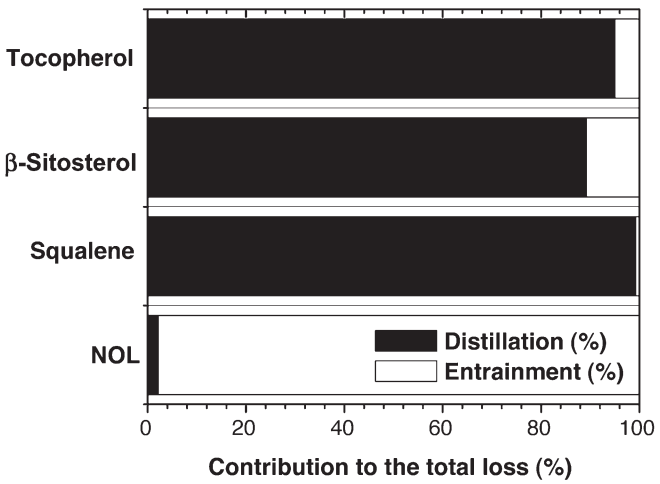

FIG. 3. Contribution of distillative and entrainment effects to the total loss of neutral oil (NOL), squalene, β-sitosterol, and tocopherol at 2.775 mm Hg, 250°C, and 1.3% of stripping steam.

from our simulations, except for squalene. Even though the conditions selected for our work (see Table 3) covered a common range of operating pressures and temperatures, some combinations might be not usual (258°C and 1 mm Hg, or 242°C and 6 mm Hg). For example, in our simulations the highest concentration of acylglycerols (TAG, DAG, and MAG) in the distillate was obtained at the condition of 258°C and 1 mm Hg, but in industrial practice this temperature would be combined with a pressure nearer to 5 mm Hg (31). Note also that, in this case, the ratio of acid value to saponification value was equal to 0.55, which indicates excess neutral oil in the distillate (31). However, this first comparison permits one to observe that our deodorizer modeling gave satisfactory results. In particular, in the case of the tocopherol content in the deodorized oil, a very good comparison can be made with the work of Maza *et al.* (16).

Maza *et al.* (16) studied the effect of deodorization parameters (temperature and oil flow rate) on tocopherol retention using response surface methodology (RSM), which allowed the development of an equation (Eq. 11) correlating this important quality factor to process conditions (oil flow rate and temperature). In their work, a plant continuous deodorizer was used. Table 5 shows the values reported by Maza *et al.* (16) and the results of our simulations. The estimated values using their equation are also shown. It is important to highlight that Equation 11 is valid for any combination in the range of the temperatures and oil flow rates studied.

$$TOCO_r(\%) = 821.255 - 12.840 \cdot r - 1.569 \cdot t + 0.028 \cdot t \cdot r \quad R^2 = 0.997 \quad [11]$$

where $TOCO_r$ (%) is the tocopherol retention, r is the oil throughput rate (1,000 lb/h), and t is the deodorization temperature (°F).

As one can see in Table 5, there is very good agreement between the experimental values for tocopherol content from Maza *et al.* (16) and our work. The greatest difference was equal to 108 mg/kg (40,000 lb/h and 500°F), whereas the lowest difference was only 23 mg/kg (50,000 lb/h and 500°F), corresponding to 10.1 and 2.0% of deviation, respectively. In general, very good tocopherol retention values were achieved by Maza *et al.* (16). Our simulations always gave higher values than the experimental ones, although they were not so high as the ones calculated using Equation 11 suggested by Maza *et al.* (16). Since Equation 11 was obtained from a statistical procedure (RSM), it is possible to say that there was no significant difference between our tocopherol levels and theirs. We should highlight that, for the simulation results given in Table 5, all processing conditions (P, T, and % steam) and initial concentrations of tocopherol in the oil to be deodorized were given by Maza *et al.* (16). In this way, our simulation program was capable of reproducing them faithfully and generating agreeable results. In the case of the final FFA content, our work generated lower values. One possible explanation is the absence of hydrolytic reactions. Nevertheless, it is noteworthy that only one value (500°F and 40,000 lb/h) was lower than 0.005%, which was taken as the minimum final FFA level when steam was used for stripping (1). In general, both tocopherol and FFA contents decreased with temperature (became more volatile) and increased with oil flow rate. From a statistical analysis of the results in Table 5, it was possible to conclude that temperature had the main effect on tocopherol retention in the oil, which is in accordance with the work of Walsh *et al.* (31).

To further show the applicability of our methodology, we investigated the deodorization of canola oil, which differs from soybean and wheat germ oils because of its high content of oleic acid (61%; see Table 1). The simulation results for the composition of deodorizer distillate were compared with the work of Verleyen *et al.* (4). The authors reported two different results for the composition of deodorizer distillates from canola oil (shown in parentheses in the next sentence). At 240°C and 4 mm Hg with 1.3% of stripping steam, the distillate (in a free basis of water) contained 6.5% of β-sitosterol (4.0 and 6.2%), 4.1% of tocopherol (3.7 and 4.2%), 2.1% of MAG (1.4 and 2.1%), 2.2% of DAG (3.8 and 3.9%), and 2.8% of TAG (3.0 and 7.5%). Verleyen *et al.* (4) called attention to the strong relation linking tocopherol and sterol contents in the deodorizer distillate, the initial FFA content in the oil, and the deodorization process conditions applied (including temperature, steam rate, and pressure). We explored our simulation tool to investigate these relations. Reducing the initial FFA content from 0.1 to 0.05% while maintaining the concentrations of other minor compounds (see Table 1) and the aforementioned processing conditions (240°C, 4 mm Hg, and 1.3% of stripping steam) increased the contents of β-sitosterol and tocopherol in the distillate to 11.0 and 7%, respec-

TABLE 5
Effects of Deodorization Conditions on Final Oil Acidity and Tocopherol Retention in Soybean Oil

	Maza *et al.* (16)						This work[a]								
Temperature (°F)	475		488		500		475			488			500		
Oil flow rate (1,000 lb/h)	40	50	45	45	40	50	40	45	50	40	45	50	40	45	50
Tocopherol (mg/kg)	1,150	1,190	1,110	1,120	1,000	1,130	1,220	1,235	1,247	1,169	1,188	1,204	1,108	1,133	1,153
Tocopherol retention (%)	84.6	87.5	81.6	82.4	73.5	83.1	89.7	90.8	91.7	86.0	87.3	88.5	81.5	83.3	84.8
Tocopherol retention[b] (%)	94.4	99.0	92.8	92.8	83.2	94.8	94.4	96.7	99.0	88.8	92.8	96.9	83.2	89.0	94.8
Oil acidity[c] (%)	0.020	0.024	0.018	0.018	0.014	0.017	0.009	0.011	0.012	0.006	0.007	0.008	0.004	0.004	0.005

[a]Murphree efficiencies were considered.
[b]Estimated using the equation of Maza *et al.* (16); see Equation 11. Initial tocopherol content of 1,360 mg/kg.
[c]Expressed as the percentage of oleic acid (% C18:1) in the deodorized oil.

tively. The same behavior occurred when increasing the steam rate to 2% (4 mm Hg and 240°C, initial concentrations as in Table 1). In this case, the contents of β-sitosterol and tocopherol in the distillate rose to 8.0 and 5.1%, respectively

Because our simulation program permitted the investigation of different flow patterns, we studied the effect of countercurrent (Fig. 1B) and cross-flow (Fig. 1A) configurations on the composition of the product streams. At 250°C, 1.3% of stripping steam, and 2.775 mm Hg, the main differences encountered were in the final oil acidity and tocopherol content. In comparison with the values found for the cross-flow deodorizer (see Table 4), the countercurrent deodorizer generated a lower level of FFA (0.0028%), which was three times less, and a superior tocopherol content (1,361 mg/kg), which was 12% higher. Even with the bottom pressure almost twice the top pressure (due to the pressure drop), irrelevant changes were generated in the distillate composition. These differences could be due to column configuration (cross-flow and countercurrent) and/or the pressure drop. However, as shown in Table 6, when the pressure drop in the countercurrent pattern was not considered, an even lower final acidity was generated whereas NOL and tocopherol values were not affected.

On the subject of the VLE approach adopted in this work, a careful analysis of the calculated values of ϕ_i^{sat}, ϕ_i, and POY for all components, including water, was done to explain the use of vapor phase nonidealities even at very low pressures. ϕ_i^{sat} values differentiated considerably from unity ($\phi_i^{sat} < 0.89$) for water, whereas ϕ_i and POY values were virtually one (>0.997) for all components in the system. This was a consequence of the high values of water vapor pressures calculated at the high temperatures observed in the deodorizer. The vapor pressure was a parameter that was used in the calculation of ϕ_i^{sat}. For simplification, it is possible to consider ϕ_i and POY as equal to one, and ϕ_i^{sat} only for water in the calculation of the VLE.

The main effect related to the inclusion of Murphree efficiencies within the deodorizer was the increase in final oil acidity. In this case, more stages would have been necessary to achieve the same final content. This is in accordance with the definition of Murphree efficiency, i.e., that as it approaches unity, the mass transfer of the oil components (FFA, for example) from the liquid to the vapor phase is more efficient, depleting their concentration in the oil.

TABLE 6
Comparison Between Cross-flow and Countercurrent Flow in Multitray Deodorizers

	2.775 mm Hg and 250°C		
		Countercurrent flow (Fig. 1B)	
Quality	Cross-flow (Fig. 1A)	With pressure drop[a]	Without pressure drop
Oil acidity (%)	0.0088	0.0028	0.0017
Tocopherol in the oil (mg/kg)	1,216	1,361	1,361
NOL (%)	0.01	0.02	0.02
Distillate (kg/h)	4.96	3.97	4.17

[a]Bottom pressure of 4.775 mm Hg. For other abbreviation, see Table 4.

For wheat germ oil deodorization, we were able to make a qualitative comparison with the experimental work of Wang and Johnson (5) by using the configuration from Figure 1B and the processing conditions given in Table 3. The simulation results indicate that at 200°C, there were 2,454 and 2,431 mg/kg of tocopherol in the oil deodorized at 25 and 10 mL/min of oil flow rate, respectively. At 250°C, these values were 2,230 and 1,874 mg/kg, in that order. The oil flow rate (related to residence time) did not affect tocopherol content considerably for lower temperatures but had an important effect at higher ones. Both temperature and oil flow rate had an impact on the final oil acidity. At 25 mL/min, the increase in temperature, from 200 to 250°C, changed the final FFA content from 0.120 to 0.001%. At 10 mL/min, this change was even greater. For the conditions studied, the tocopherol reduction varied from 0.6 (200°C and 25 mL/min) to 24.1% (250°C and 10 mL/min). NOL values increased with temperature and decreased with oil flow rate (2.05% for 10 mL/min and 250°C, and 0.62% for 25 mL/min and 200°C). Because the complete oil composition used as a feed stream in some of the deodorization experiments performed by Wang and Johnson (5) was not available, a quantitative comparison was not possible. But from a qualitative point of view, they also found that to reduce FFA efficiently while maintaining the tocopherol in the oil, it is better to use lower temperatures and oil flow rates.

The multicomponent stripping column modeling proposed in this work permitted the simulation of oil-refining processes performed under vacuum at high temperatures, as deodorization and deacidification by steam refining. Despite the good agreement with experimental results, some limitations should be considered. Our modeling needs several physical properties to describe enthalpy balances and equilibrium relationships, in combination with methods to estimate entrainment and Murphree efficiencies. Some of the required properties are often difficult to determine experimentally because of the complexity of the mixture, diversity of the compounds, and range of operating conditions (high temperatures, for example). To overcome this limitation, we adopted shortcuts, such as the use of predictive methods for the cases where empirical equations were not available and the application of methods developed for other kinds of industry equipment to deodorizers (entrainment and Murphree efficiency, for example). We should highlight that the procedures and methods selected for estimating physical properties and other process parameters play an important role in the calculations, i.e., there is a direct relation between the predictive capacity of the selected methods and the results given by the simulation program. Further improvements, especially concerning the methods for estimating entrainment and Murphree efficiencies for deodorizers, might enhance the applicability of this simulation tool in the edible oil industry. Also, chemical reaction effects, such as FA generation (from hydrolysis of acylglycerols) and FA isomerization, were not considered and have an impact in the final results (oil acidity, for example). Such aspects should be included in a future work.

With the tools provided by Ceriani and Meirelles (10), phase equilibria can be rigorously calculated. The software developed in the present work takes into account the detailed oil compositions and includes Murphree efficiencies and entrainment effects, so it can be used to analyze the effects of possible operating conditions and help guiding industrial and experimental works. Despite the necessary shortcuts that must be done, process simulation, together with experimental work and industrial knowledge, can lead to an efficient process development and optimization.

ACKNOWLEDGMENTS

The authors wish to acknowledge FAPESP (Fundação de Amparo à Pesquisa do Estado de São Paulo–03/04949-3) and CNPq (Conselho Nacional de Desenvolvimento Científico e Tecnológico–521011/95-7) for financial support. The authors also thank Dr. Tong Wang, who contributed important information about her work.

APPENDIX I: EQUATIONS FOR THE CONTINUOUS MULTITRAY COUNTERCURRENT FLOW DESIGN

For an arbitrary stage n of a stripping column, the related nomenclature can be set as follows.

Subscript n: flow from stage n, $n = 1, 2, \ldots, NS$; subscript i: component i, $i = 1, 2, \ldots, NC$; H = vapor phase enthalpy (J/h); h = liquid phase enthalpy (J/h); h_f = liquid feed enthalpy (J/h); H_f = vapor feed enthalpy (J/h); V = total vapor flow (mol/h); v = component vapor flow (mol/h); L = total liquid flow (mol/h); l = component liquid flow (mol/h); f = component feed flow as liquid (mol/h); F = component feed flow as vapor (mol/h).

For each stage n, a set of dependent relationships (test functions $F_{k(n,i)}$) must be satisfied. In the equations below, the entrainment term (e_n) is already introduced.

Component balances (total: $NS \times NC$ relations):

$$F_{1(n,i)} = l_{n,i} + v_{n,i} + V_n \cdot e_n \cdot \frac{l_{n,i}}{L_n} - v_{n-1,i} - V_{n-1} \cdot e_{n-1} \cdot \frac{l_{n-1,i}}{L_{n-1}} - l_{n+1,i} - f_{n,i} - F_{n,i} = 0 \quad [A1]$$

Enthalpy balances (total: NS relations)

$$F_{2(n)} = h_n + H_n + e_n \cdot V_n \cdot \frac{h_n}{L_n} - H_{n-1} - e_{n-1} \cdot V_{n-1} \cdot \frac{h_{n-1}}{L_{n-1}} - h_{n+1} - h_{f,n} - H_{f,n} = 0 \quad [A2]$$

Equilibrium conditions derived from the definitions of the vapor-phase Murphree plate efficiency, $\eta_{n,i}$ (total: $NS \times NC$ relations):

$$F_{3(n,i)} = \eta_{n,i} \cdot K_{n,i} \cdot V_n \cdot \frac{l_{n,i}}{L_n} - v_{n,i} + (1 - \eta_{n,i}) \cdot v_{n-1,i} \cdot \frac{V_n}{V_{n-1}} = 0 \quad [A3]$$

The above relationships comprise a vector of test functions,

$$\mathbf{F}(\mathbf{x}) = \{\mathbf{F_1};\mathbf{F_2};\mathbf{F_3}\} = 0 \quad [A4]$$

that contains NS ($2NC + 1$) elements, and that may be solved for equally many unknowns:

$$\mathbf{x} = \{\mathbf{l};\mathbf{v};\mathbf{t}\} = 0 \quad [A5]$$

where the vector $\mathbf{l}$ contains all the elements $l_{n,i}$, $\mathbf{v}$ all the elements $v_{n,i}$, and $\mathbf{T}$ all elements T_n.

Once $l_{n,i}$, $v_{n,i}$, and T_n are known, the product compositions, the product flow rates, the concentrations, and the temperature profiles in the column follow readily. The iterative Newton–Raphson method solves Equation A4 using the prior set of values of the independent variables (Eq. A5). A first estimate is necessary to initiate the calculations.

APPENDIX II: EQUATIONS FOR THE CONTINUOUS MULTITRAY CROSS-FLOW DESIGN

Component balances (total: $NS \times NC$ relations):

$$F_{1(n,i)} = l_{n,i} + v_{n,i} + V_n \cdot e_n \cdot \frac{l_{n,i}}{L_n} - l_{n+1,i} - f_{n,i} - F_{n,i} = 0 \quad [A6]$$

Enthalpy balances (total: NS relations)

$$F_{2(n)} = h_n + H_n + e_n \cdot V_n \cdot \frac{h_n}{L_n} - h_{n+1} - h_{f,n} - H_{f,n} = 0 \quad [A7]$$

Equilibrium conditions derived from the definitions of the vapor phase Murphree plate efficiency, $\eta_{n,i}$ (total: $NS \times NC$ relations):

$$F_{3(n,i)} = \eta_{n,i} \cdot K_{n,i} \cdot V_n \cdot \frac{l_{n,i}}{L_n} - v_{n,i} + (1 - \eta_{n,i}) \cdot V_n \cdot \frac{F_{n,i}}{\sum_i F_{n,i}} = 0 \quad [A8]$$

REFERENCES

1. Carlson, K.F., Deodorization, in *Bailey's Industrial Oil and Fat Products*, 5th edn., edited by Y.H. Hui, Wiley-Interscience, New York, 1996, Vol. 4, pp. 339–390.
2. Woerfel, J.B., Soybean Oil Processing By-products and Their Utilization, in *Practical Handbook of Soybean Processing and Utilization,* edited by D.R. Erickson, AOCS Press, Champaign, 1995, pp. 306–313.
3. Ahrens, D., Comparison of Tray, Thin-Film Deodorization, *INFORM 9*:566–576 (1998).
4. Verleyen, T., R. Verhe, L. Garcia, K. Dewettinck, A. Huyghebaert, and W. De Greyt, Gas Chromatographic Characterization of Vegetable Oil Deodorization Distillate, *J. Chromatogr. A 921*:277–285 (2001).
5. Wang, T., and L.A. Johnson, Refining High-Free Fatty Acid Wheat Germ Oil, *J. Am. Oil Chem. Soc. 78*:71–76 (2001).
6. Naphtali, L.M., and D.P. Sandholm, Multicomponent Separation Calculations by Linearization, *AIChE J. 17*:148–153 (1971).
7. Pryde, E.H., Composition of Soybean Oil, in *Practical Handbook of Soybean Processing and Utilization,* edited by D.R. Erickson, AOCS Press, Champaign, 1995, pp. 13–31.

8. Firestone D., *Physical and Chemical Characteristics of Oils, Fats and Waxes*, AOCS Press, Champaign, 1999, 152 pp.
9. Balchen, S., R. Gani, and J. Adler-Nissen, Deodorization Principles, *INFORM 10*:245–262 (1999).
10. Ceriani, R., and A.J.A. Meirelles, Predicting Vapor–Liquid Equilibria of Fatty Systems, *Fluid Phase Equilib. 215*, 227–236 (2004).
11. Fornari, T., S. Bottini, and E.A. Brignole, Application of UNIFAC to Vegetable Oil–Alkane Mixtures, *J. Am. Oil Chem. Soc. 71*:391–395 (1994).
12. Antoniosi Filho, N.R., O.L. Mendes, and F.M. Lanças, Computer Prediction of Triacylglycerol Composition of Vegetable Oils by HRGC, *J. Chromatogr. 40*:557–562 (1995).
13. Rabelo, J., E. Batista, F.W. Cavaleri, and A.J.A. Meirelles, Viscosity Prediction for Fatty Systems. *J. Am. Oil Chem. Soc. 77*:1255–1261 (2000).
14. Ceriani, R., and A.J.A. Meirelles, Simulation of Batch Physical Refining and Deodorization Processes, *Ibid. 81*:305–312 (2004).
15. Petrauskaitè, V., W.F. De Greyt, and M.J. Kellens, Physical Refining of Coconut Oil: Effect of Crude Oil Quality and Deodorization Conditions on Neutral Oil Loss, *Ibid. 77*:581–586 (2000).
16. Maza, A., R.A. Ormsbee, and L.R. Strecker, Effects of Deodorization and Steam-Refining Parameters on Finished Oil Quality, *Ibid. 69*:1003–1008 (1992).
17. Barnes, P.J., Lipid Composition of Wheat Germ and Wheat Germ Oil, *Fette Seifen Anstrichm. 84*:256–268 (1982).
18. Eskin, N.A.M., B.E. McDonald, R. Przybylski, L.J. Malcolmson, R. Scarth, T. Mag, K. Ward, and D. Adolph, Canola Oil, in *Bailey's Industrial Oil and Fat Products*, 5th edn., edited by Y.H. Hui, Wiley-Interscience, New York, 1996, Vol. 2, pp. 1–95.
19. Reid, R.C., J.M. Prausnitz, and B.E. Poling, *The Properties of Gases and Liquids*, McGraw-Hill, New York, 1987.
20. Tu, C.H., and C.P. Liu, Group-Contribution Estimation of the Enthalpy of Vaporization of Organic Compounds, *Fluid Phase Equilib. 121*:45–65 (1996).
21. DIPPR Student Chemical Database, http://dippr.byu.edu/students/chemsearch.asp (accessed April 2003).
22. Voutsas, E., M. Lampadariou, K. Magoulas, and D. Tassios, Prediction of Vapor Pressures of Pure Compounds from Knowledge of the Normal Boiling Point Temperature, *Fluid Phase Equilib. 198*:81–93 (2002).
23. Retzekas, E., E. Voutsas, K. Magoulas, and D. Tassios, Prediction of Physical Properties of Hydrocarbons, Petroleum and Coal Liquid Fractions, *Ind. Eng. Chem. Res. 41*:1695–1702 (2002).
24. Elbro, H.S., A. Fredenslund, and P. Rasmussen, Group Contribution Method for the Prediction of Liquid Densities as a Function of Temperature for Solvents, Oligomers and Polymers, *Ind. Eng. Chem. Res. 30*:2576–2582 (1991).
25. Bokis, C.P., C.C. Chen, and H. Orbey, A Segment Contribution Method for the Vapor Pressure of Tall-Oil Chemicals, *Fluid Phase Equilib. 155*:193–203 (1999).
26. Ludwig, E.E., *Applied Process Design for Chemical and Petrochemical Plants*, 3rd edn., GPC, Houston, 1995, Vol. 2, pp. 42–44.
27. MacFarland, S.A., P.M. Sigmund, and M. Van Winkle, Predict Distillation Efficiency, *Hydrocarbon Process. 51*:111–114 (1972).
28. Halvorsen, J.D., W.C. Mammel, and L.D. Clements, Density Estimation for Fatty Acids and Vegetable Oils Based on Their Fatty Acid Composition, *J. Am. Oil Chem. Soc. 70*:875–880 (1993).
29. Stage, H., The Physical Refining Process, *Ibid. 62:*299–307 (1985).
30. Brekke, O.L., Deodorization, in *Handbook of Soy Oil Processing and Utilization*, 4th edn., edited by D.R. Erickson, E.H. Pryde, O.L. Brekke, T.L. Mounts, and R.A. Falb, American Oil Chemists' Society, Champaign, 1980, pp. 155–191.
31. Walsh, L., R.L. Winters, and R.G. Gonzalez, Optimizing Deodorizer Distillate Tocopherol Yields, *INFORM 9*:78–83 (1998).

[Received June 23, 2004; accepted October 15, 2004]